[논 문] 한국재료학회지
Kor. J. Mater. Res.
Vol. 19, No. 4 (2009)

DOI: 10.3740/MRSK.2009.19.4.203

Phase Change Characteristics of Sn_XSe_{100-X} Thin Films by RF-magnetron Sputtering

Sang Kyun Kim and Se-Young Choi†

Department of Materials Science and Engineering, Yonsei University, 134 Shinchondong, Seodaemungu, Seoul 120-749, Korea

(Received December 20, 2008 : Received in reviced form January 5, 2009 : Accepted March 9, 2009)

Abstract Sn_XSe_{100-X} ($15 \le X \le 30$) alloys have been studied to explore their suitability as phase change materials for nonvolatile memory applications. The phase change characteristics of thin films prepared by a Radio Frequency (RF) magnetron co-sputtering system were analyzed by an X-ray diffractometer and 4-point probe measurement. A phase change static tester was also used to determine their crystallization under the pulsed laser irradiation. X-ray diffraction measurements show that the transition in sheet resistance is accompanied by crystallization. The amorphous state showed sheet resistances five orders of magnitude higher than that of the crystalline state in Sn_XSe_{100-X} ($x = 15, 20, 25, 30$) films. In the optimum composition, the minimum time of Sn_XSe_{100-X} alloys for crystallization was 160, 140, 150, and 30ns at 15mW, respectively. The crystallization temperature and the minimum time for crystallization of thin films were increased by increasing the amount of Sn, which is correlated with the activation energy for crystallization.

Key words phase change materials, SnSe thin film, Se based materials, PRAM.

1. Introduction

Phase change materials, namely chalcogenides,[1] enabled data storage such as optical mass storage device and phase change random access memory (PRAM)[2] by using its optical or electrical switching property upon phase transition. Due to the rapid switching between the amorphous and crystalline states, PRAM is considerably faster than flash memory by more than ten times and could be even less expensive in production because of its simple fabrication technology and structure.[3] The drastic drop of sheet resistance based on the percolation which is the process forming electrical conducting channel during crystallization.[4] PRAM is equipped with great potentials such as low power, high speed, robust durability, and non-volatility. However, such applications still demand advanced materials to guarantee high speed, low power consumption and reliability of device, which could be realized by control of phase transition behaviors such as rapid crystallization, easy amorphization, and reinforced phase stability of phase change materials. There has been relatively less work done on SnSe thin films grown by magnetron sputtering. In this study, we report on the structural and electrical properties of Sn_XSe_{100-X} films.

†Corresponding author
E-Mail : sychoi@yonsei.ac.kr (S. -Y. Choi)

2. Experimental Procedure

Sn_XSe_{100-X}($x = 15, 20, 25, 30$) films were deposited by radio frequency magnetron co-sputtering system (SNTek, Korea) on Si (100) wafers and slide glasses by using Sn (99.99%, RND KOREA, Korea) and Se (99.997%, RND KOREA, Korea). The base pressure was 5×10^{-7} Torr and working pressure was adjusted to 1.5 mTorr by flowing Ar (6N, Seoul gas, Korea) through a mass flow controller. Deposition rate of films was controlled by applying different RF-power to each target. Targets were pre-sputtered for 10 minutes in order to remove oxidized surface and contaminations. The substrate holder was rotated at 20 rpm for homogenization of the thin film thickness and composition. As-deposited films were annealed in Ar atmosphere for 10 min at 100~350 °C at a heating rate of 5 K/min. The crystal structure was analyzed by X-ray diffractometer (Rigaku D/MAX II A, Japan & Philips X'pert MRD, Philips, Netherlands). The phase transition behavior was observed by laser irradiation using a static tester (Nanostorage Co. Ltd., KOREA) in nanosecond scale.

3. Results and Discussion

3.1 Phase transition characteristics

Fig. 1 shows XRD patterns of Sn_XSe_{100-X} with different

composition ratio and annealing temperatures. All Sn_XSe_{100-X} alloys show the presence of the broad peak in the as-deposited state.

This is a typical property of an amorphous phase. As deposited SnSe films are at amorphous states, as Se might have reinforced the amorphous stability of films. The XRD spectra of crystalline SnSe films show an increase in the intensity of the (111) peak with increasing amount of Sn. This could possibly be explained by the decrease in surface free energy.[5)]

3.2 Sheet resistance of SnSe alloys

Fig. 2 presents the temperature dependent sheet resistances of 200 nm Sn_XSe_{100-X} with different composition

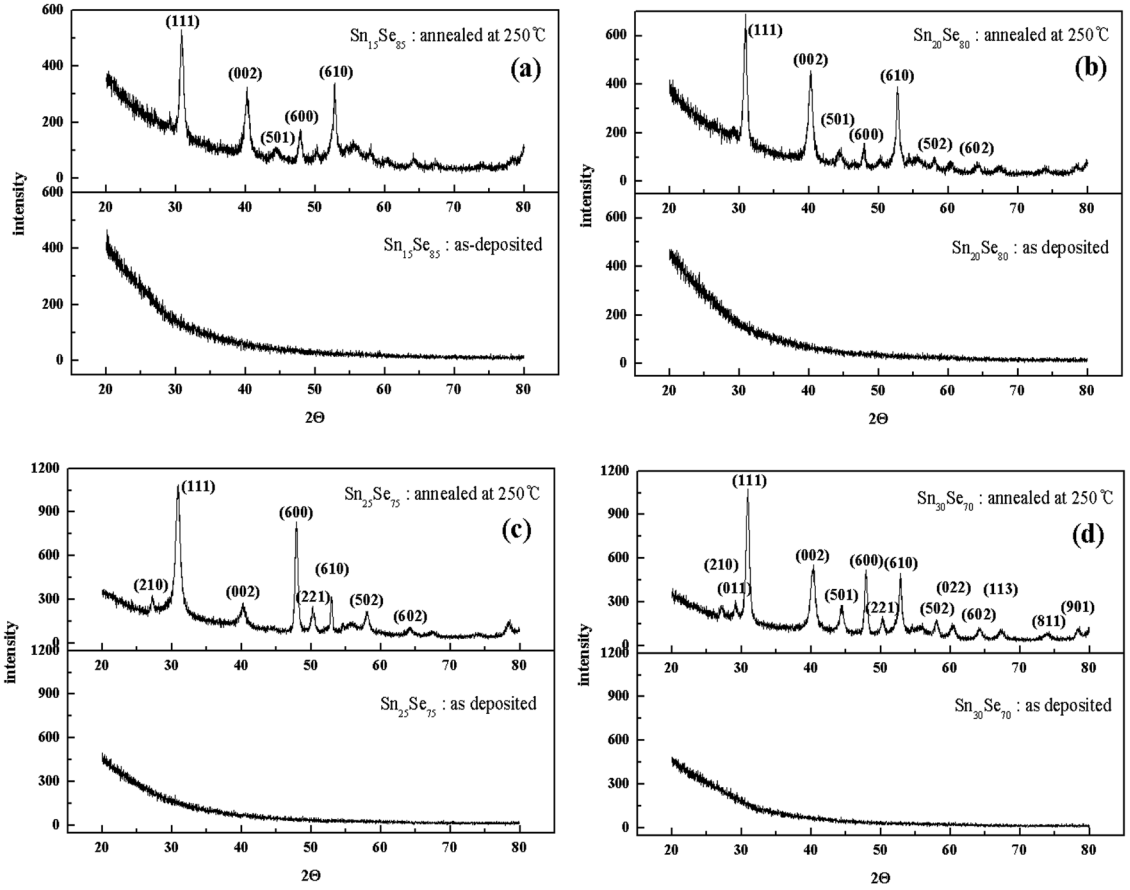

Fig. 1. XRD patterns of (a) $Sn_{15}Se_{85}$, (b) $Sn_{20}Se_{80}$, (c) $Sn_{25}Se_{75}$ and (d) $Sn_{30}Se_{70}$ annealed at 250°C.

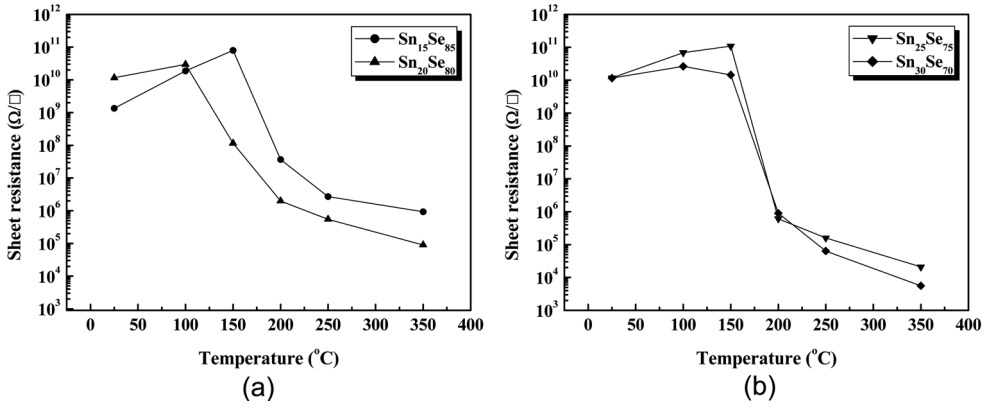

Fig. 2. Temperature dependent sheet resistance of (a) Sn_XSe_{100-X} (x = 15, 20) and (b) Sn_XSe_{100-X} (x = 25, 30) with different SnSe composition ratio and annealing temperatures.

ratio and annealing temperatures. At room temperature, all Sn_XSe_{100-X} films were amorphous. The sheet resistance of $Sn_{25}Se_{75}$ was $1.17\times10^{10}\,\Omega/\square$ at room temperature and decreased to $6.1\times10^{5}\,\Omega/\square$ upon annealing at 250 °C. The sheet resistances of $Sn_{15}Se_{85}$, $Sn_{20}Se_{80}$ thin films at room temperature were about 1.3×10^{9} and $1.2\times10^{10}\,\Omega/\square$, respectively. However, they decreased slowly to about $2K\Omega/\square$ after crystallization. The smooth decrease of sheet resistance in the region between 150 and 250 °C might be based on the crystal growth which strengthened conducting channel and decreased sheet resistance.[6] As the amount of Sn increased, phase transition temperature increased but phase thermal stability was improved. Also, the margin of resistance between amorphous and crystalline Sn_XSe_{100-X} (X = 25, 30) thin films was increased. The decrease in sheet resistance upon annealing for Sn_XSe_{100-X} film is indicative of a semiconductor like behavior in the crystalline state.[7]

3.3 Crystallization behavior

To investigate the phase transition behavior in the scale of nano-seconds, static tester was employed. Fig. 3 depicts the PTE (Power-Time-Effect) diagram[8] of Sn_XSe_{100-X} films, which reveals reflectivity with laser conditions. The reflectivity change, optical contrast (△R) is defined by the following equation: $\triangle R = (R_{after}-R_{before})/R_{before}$, where R_{before} and R_{after} indicate the reflectivity before and after irradiation, respectively. The magnitude of △R is illustrated by different colors in the PTE diagram. 1st blue region presents that there were no changes of △R since the condition of applied laser was insufficient for crystallization. When the laser power or pulse width increased, red region presents that reflectivity changes upon crystallization.

In the case of $Sn_{30}Se_{70}$ film, relatively fast and easy crystallization occurred with short pulse width and low laser power. However, other films were hard to crystallize. At high laser power and long pulse width, ablation (2nd blue region) did occur. It means that $Sn_{30}Se_{70}$ alloys exhibit a small extent of thermal insta-bility.

Fig. 4 depicts △R (reflectivity changes) of Sn_XSe_{100-X} at 10, 15, and 20 mW, respectively. Reflectivity changed due to crystallization and ablation. Under the laser irradiation, △R was changed owing to the phase transformation. The minimum time for crystallization of $Sn_{15}Se_{85}$, $Sn_{20}Se_{80}$, $Sn_{25}Se_{75}$ and $Sn_{30}Se_{70}$ was 160, 140, 150 and 30ns at 15 mW laser power, respectively.

In addition, the $Sn_{30}Se_{70}$ sustained large △R with rapid crystallization, which presented △R up to 0.289. Sn accelerated the crystallization time of thin films.

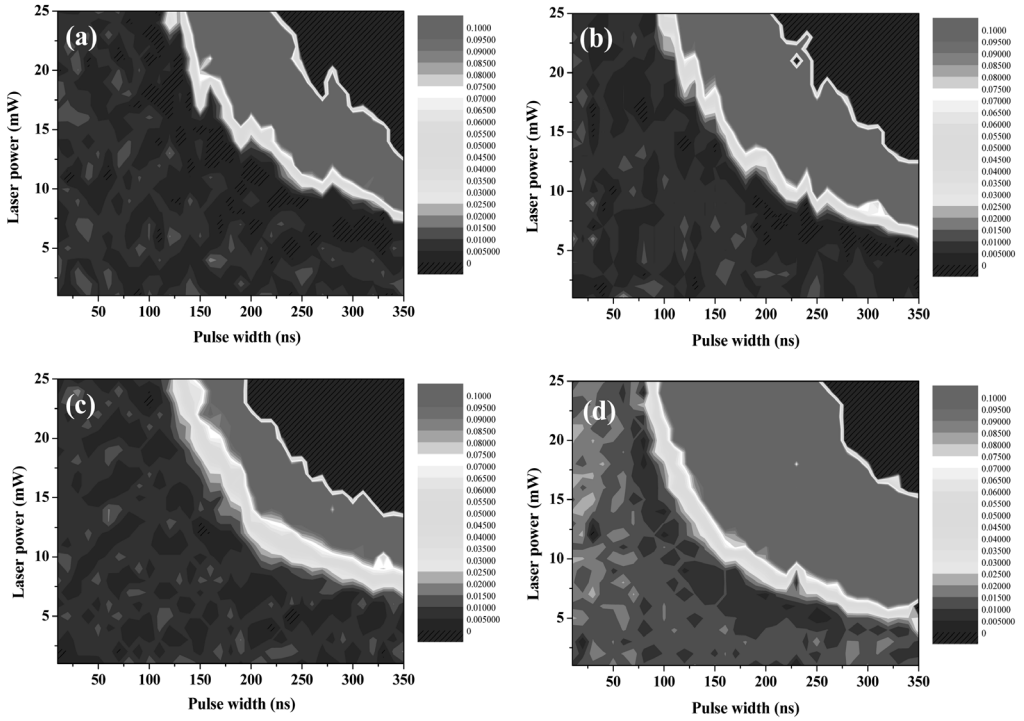

Fig. 3. PTE diagram of (a) $Sn_{15}Se_{85}$, (b) $Sn_{20}Se_{80}$, (c) $Sn_{25}Se_{75}$ and (d) $Sn_{30}Se_{70}$ with different laser power and pulse width.

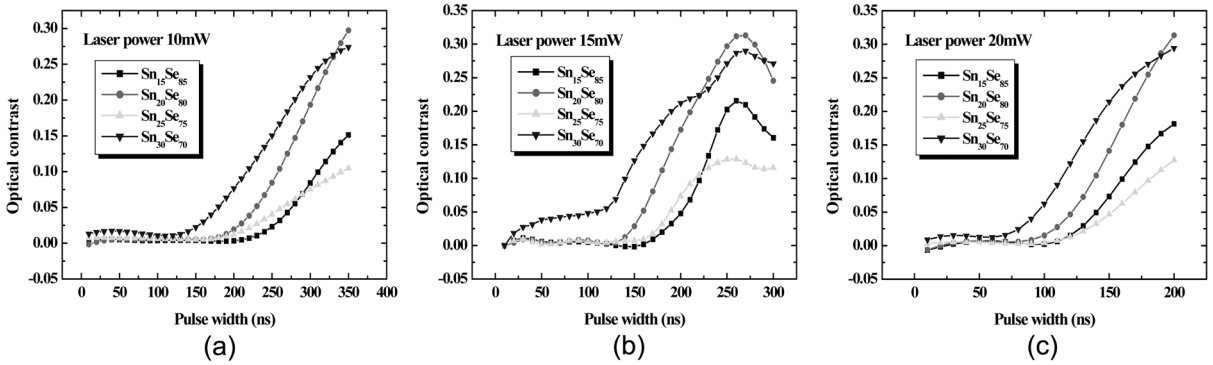

Fig. 4. Time dependent optical contrast of $Sn_{15}Se_{85}$, $Sn_{20}Se_{80}$, $Sn_{25}Se_{75}$ and $Sn_{30}Se_{70}$ with (a) 10, (b) 15, (c) 20mW laser power.

However, except for $Sn_{30}Se_{70}$ film, other films were hard to crystallize. The ablation of Sn_XSe_{100-X} films appeared at 250ns with 15mW laser power. From these results, $Sn_{30}Se_{70}$ can be considered as a material exhibiting rapid phase transformation and low power consumption during device operation. From these results, we can conclude that $Sn_{30}Se_{70}$ is a useful candidate as a material of enhanced phase stability.

4. Conclusion

In this study, Se result in high crystallization temperature meaning that selenium might have acted as amorphous stabilizers. Crystallization of $Sn_{30}Se_{70}$ film was carried out in a short time. Furthermore, the difference in sheet resistance between amorphous and crystalline states was more than 5 orders of magnitude. When doing a unit conversion, this alloy has a higher resistivity in the crystalline state compared with the resistivity of reference materials such as Sb based. This indicates that $Sn_{30}Se_{70}$ film could possibly minimize the reset current of PRAM devices. Therefore, $Sn_{30}Se_{70}$ would contribute to fast operation and low power consumption device in PRAM application.

Acknowledgment

This work was supported by the Second Stage of Brain Korea 21 Project in 2008.

References

1. R. Bez, A. Pirovano, Mater. Sci. Semicond. Process., **7**, 349 (2004).
2. A. L. Lacaita, Solid-State Electron., **50**, 24 (2006).
3. K. N. Kim and G.. T. Jeong, Microsyst. Technol., **13**, 145 (2007).
4. D. Kim, F. Merget, M. Laurenzis, P. H. Bolivar, and H. Kurz, J. Appl. Phys., **97**, 083538 (2005).
5. K.-M. Chung, D. Wamwangi, M. Woda, M. Wuttig and W. Bensch, J. Appl. Phys., **103**, 083523 (2008).
6. M. J. Kang, S. Y. Choi, D. Wamwangi, K. Wang, C. Steimer and M. Wuttig, J. Appl. Phys., **98**, 014904 (2005).
7. S. R. Ovshinsky, Phys. Rev. Lett., **21**, 1450 (1968).
8. S.-J. Park, I. S. Kim, S.-K. Kim, Kor. J. Mater. Res., **18**, 2 (2008).